

4H-SiC photoconductive switching devices for use in high-power applications

S. Doğan,^{a)} A. Teke,^{b)} D. Huang, and H. Morkoç

Department of Electrical Engineering, Virginia Commonwealth University, 601 W. Main Street, Richmond, Virginia 23284

C. B. Roberts

Tech Explore, Limited Liability Corporation, 5273 College Corner Pike No. 12, Oxford, Ohio 45056

J. Parish and B. Ganguly

Air Force Research Laboratory, Wright-Patterson Air Force Base, Ohio 45433

M. Smith, R. E. Myers, and S. E. Saddow

Electrical Engineering University of South Florida, Tampa, Florida 33543

(Received 12 December 2002; accepted 10 March 2003)

Silicon carbide is a wide-band-gap semiconductor suitable for high-power high-voltage devices and it has excellent properties for use in photoconductive semiconductor switches (PCSSs). PCSS were fabricated as planar structures on high-resistivity 4H-SiC and tested at dc bias voltages up to 1000 V. The typical maximum photocurrent of the device at 1000 V was about 49.4 A. The average on-state resistance and the ratio of on-state to off-state currents were about 20 Ω and 3×10^{11} , respectively. Photoconductivity pulse widths for all applied voltages were 8–10 ns. These excellent results are due in part to the removal of the surface damage by high-temperature H₂ etching and surface preparation. Atomic force microscopy images revealed that very good surface morphology, atomic layer flatness, and large step width were achieved. © 2003 American Institute of Physics. [DOI: 10.1063/1.1571667]

Silicon carbide (SiC), a wide-band-gap semiconductor of ~ 3 eV, is a candidate material for electronic and optical devices and has advantages over other semiconductors especially for high-frequency, high-temperatures and high-power applications.¹ This is because of its high saturation electron velocity (2.0×10^7 cm/s), thermal conductivity (4.9 W/cm °C), and high breakdown field (4 MV/cm).^{2,3} The large band gap and high saturation electron velocity of SiC provide excellent high-temperature stability and high-frequency performance for various device applications.⁴ For that reason, SiC technology has made tremendous improvements in the last decade with a variety of encouraging device and circuit demonstrations.⁵

SiC-based semiconductor electronic devices and circuits are presently being developed for use in high-power, high-temperature, and high radiation conditions in which conventional semiconductors can not adequately perform. The photoconductive semiconductor switch (PCSS) is an important type of electronic device and excels in applications requiring high voltage and high speed. Some of the applications of the PCSS include high-speed photodetectors, high-voltage pulse generation, and electron-beam pumped lasers, and radio frequency interference immunity. There is strong interest in developing these devices for use in high-power and high-temperature applications. PCSSs have unique advantages over conventional power switches including high breakdown

field, high speed, long lifetime, and negligible jitter time. Although Si and GaAs are the most commonly used materials in PCSS,^{6,7} compared to GaAs and Si, better performance and wider (more) applications are expected from SiC PCSS due to its higher saturation electron drift velocity and higher thermal conductivity. The advantages of PCSSs over conventional switches make them the perfect choice for many important applications where high switching accuracy and power capability are important. Furthermore, wide-band-gap semiconductor switches are attractive since they have a higher tolerance compared to other switches due to their better material properties. There has been significant interest in using high-resistivity SiC, among the wide-band-gap semiconductors, for PCSS because it is one of the most technologically advanced materials.^{8–10} In addition, PCSSs have been fabricated on SiC, both on 6H-SiC (Refs. 9 and 11) and later on 3C-SiC.¹² However, a lack of semi-insulating substrates prevented further development of PCSS technology on SiC due to the high dark currents normally encountered with less resistive substrates.

In this letter, we report measurements on 4H-SiC PCSSs for high-voltage applications. The devices were fabricated on bulk polycrystalline SiC material. These results are complemented by photoconductivity measurements under a large dc bias.

The devices were fabricated with a circular geometry with a switching gap of 1 mm on high-resistivity 4H-SiC. This relatively large device size was chosen to prevent arcing at high voltages, since the dielectric breakdown field strength of air is approximately 30 kV/cm. Since the fabricated devices are planar, the majority of the conduction will be along

^{a)}Also with Atatürk University, Faculty of Arts and Sciences, Dept. of Physics, 25240 Erzurum, Turkey; electronic mail: sdogan@vcu.edu

^{b)}Also with Balikesir University, Faculty of Arts and Sciences, Dept. of Physics, 10100 Balikesir, Turkey.

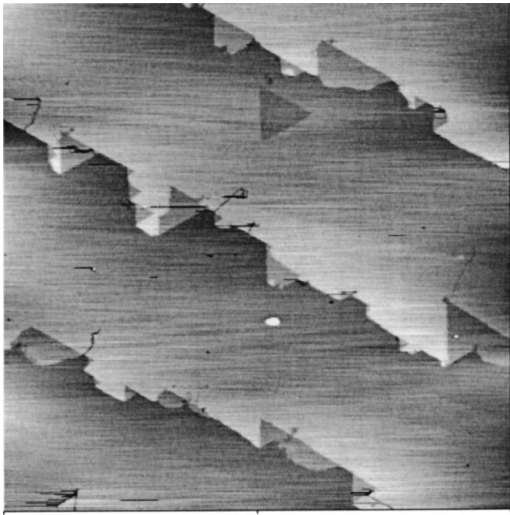


FIG. 1. AFM image from the Si face of the 4H-SiC after H_2 annealing and 15 s of molten (210°C) KOH etching. The image size is $2 \times 2 \mu\text{m}^2$. Vertical scale is 3 nm. The surface roughness (rms value) over the whole area is 0.31 nm.

the semiconductor surface. For that reason, H_2 annealing and wet KOH etching were used to passivate the surface. The surface of the SiC wafer was exposed to H_2 gas at a high temperature (1650°C) in a 10 standard liter per min (s/m) H_2 environment. This leads to surface reconstruction, where macroscopic defects, such as the damage caused by mechanical polishing, and microscopic defects on the surface are annealed out. In Fig. 1, an atomic force microscopy (AFM) image of the Si face of 4H-SiC after H_2 annealing and molten KOH etching is shown. The image size is $2 \times 2 \mu\text{m}^2$ and the vertical scale of the image is 3 nm in Fig. 1. The temperature of the molten KOH and etching time are 210°C and 15 s, respectively. The surface morphology shows atomic terraces and steps with a terrace width ranging from 0.5 to $0.8 \mu\text{m}$ and step height of ~ 1.0 nm. As can be seen in Fig. 1, the surface has atomic layer flatness. The large step width and steps are clearly observed. These terraces are due to a small misorientation of the surface direction with respect to exact (0001) or *c*-crystal direction. The step height for the 4H-SiC should be four paired atomic monolayers (MLs) corresponding to about 1.0 nm which is in agreement with the experimental observations. The terrace height on 6H-SiC should be about 6 MLs.¹³ The surface roughness [root-mean-square (rms) value] measured from this area is 0.31 nm which is small enough for device applications. These results would lead us to conclude that H_2 annealing, followed by brief KOH etching of 4H-SiC, leads to an atomically flat and damage free SiC surface, ideal for device fabrication.

The devices were fabricated in a lateral configuration with rounded contact geometries in order to minimize field enhancement effects at the corners.⁸ Following the KOH etch, chemical cleaning method, developed for Si, was used to remove the thin oxide layer from the surface of the sample. Photolithography techniques were used to define contact areas. The Ni/Ti/Au ($500 \text{ \AA} / 300 \text{ \AA} / 750 \text{ \AA}$) metalization was deposited using electron-beam (for Ni and Ti) and thermal evaporation (for Au) in order to form ohmic contacts. A standard lift-off process was applied in acetone to transfer the pattern to the sample. The contacts were an-

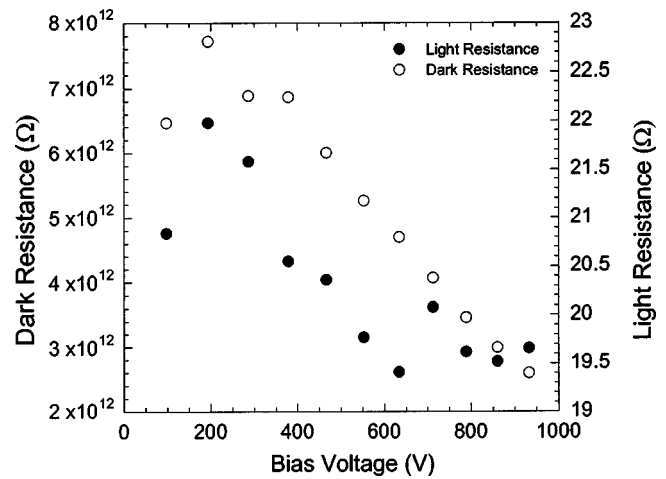


FIG. 2. SiC PCSS dark resistance vs switch voltage together with on-state switch resistance.

nealed at 950°C for 1.5 min by rapid thermal annealing in nitrogen ambient.

The photoconductivity of the SiC switches was measured under a dc bias. The photoconductive effect is based on the fact that the resistivity of a semiconductor can be altered by illuminating the material with an optical source whose photon energy is larger than the semiconductor band-gap energy, thus generating electron-hole pairs which pave the way for increased conduction. The photoconductivity measurements were performed using a frequency doubled dye laser at 307 nm (4.04 eV) with a pulse width of ~ 10 ns. A charged $0.25 \mu\text{F}$ capacitor, in parallel with the device, was used to provide a source of current during the photoconductive pulse. The voltage drop across a 10Ω current sense resistor was used to measure the photocurrent through the device, and a sensitive ammeter was put in series with the device for dark current measurements.

Figure 2 summarizes the calculated dark resistance determined from the current flowing through the switch before switching, and the switch "on" resistance versus applied the bias voltage. The resistance of the photoconductive devices can be changed over many orders of magnitude from a large value to low value in a short period of time which is comparable to the laser pulse of ~ 8 ns for fast switching. The average dark resistance of the 4H-SiC sample was $5.18 \times 10^{12} \Omega$. As can be seen from Fig. 2, the average on-state resistance is about 20Ω and the ratio of off-state to on-state resistance is about 2.5×10^{11} . The on-state switch resistance is similar to values observed by Sheng *et al.*¹²

The dependence of the dark leakage current and peak photocurrent on applied voltage for one of the devices is shown in Fig. 3. The extremely low dark leakage currents can be attributed to a low defect density in the device, but further improvements in material quality are needed. The average ratio of the peak photocurrent to dark current, which is identical to the $R_{\text{off}}/R_{\text{on}}$ resistance ratio, is 2.5×10^{11} and this is a state-of-the-art value of on/off ratio. As can be seen from Fig. 3, the peak current does not yet show saturation with applied voltage, implying that higher bias voltages can be applied to these devices. The maximum photocurrent measured at 1000 V was 49.4 A. Figure 4 summarizes the dependence of peak photocurrent on incident laser power at

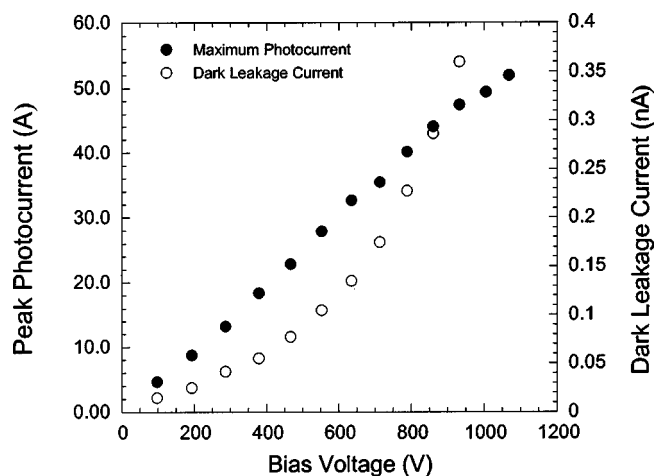


FIG. 3. The dependence of peak photocurrent and leakage current of a PCSS on applied voltage.

1005 V. The beam was attenuated, and its power measured, as each of a series of glass microscope slides were placed in the beam path. The photoconductivity experiments were then repeated with these calibrated decreases in laser pulse energy. As is seen from the inset of Fig. 4, the photocurrent saturates with increasing excitation intensity. The contact separation of the current device is 1 mm and maximum applied field is around 10 kV/cm. Since the drift velocity is about 10^6 cm/s at this value of field, the carrier transit time is about 10^{-7} s. On the other hand, the longest free carrier lifetime in SiC is attainable only in high-quality SiC layers.¹⁴ If we assume that the carrier lifetime in our bulk material were the same as in high-quality SiC, we arrive at a photoelectronic gain of about 10^{-1} which is low. It is most likely that the carrier lifetime in our bulk sample is shorter due to the density of defects, which would lower the gain even further.

The output from a commercial frequency doubled dye

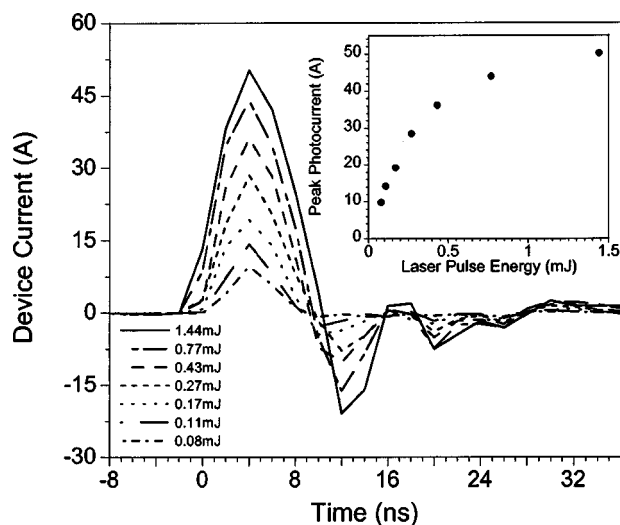


FIG. 4. Variation of photocurrent pulses with laser pulse energy. Inset shows the saturation of peak photocurrent with increasing laser pulse energy.

laser was used to measure the photoconductivity response of the PCSS. High breakdown voltage values corresponding to a high electric field have been achieved only for devices having a smaller area¹⁵ and shorter gap distance⁸ than those studied here. The electric field applied to the devices was calculated by dividing the applied voltage with the distance between contacts and was about 10 kV/cm. When the switch is illuminated, its photoconductivity will increase and current will start to flow through the current sense resistor, which gives us the observed photoconductivity response. The current should increase with increasing applied voltage until the saturation voltage is reached. The 4H-SiC PCSS tested switched the current many thousands of times and no degradation was shown on these devices at high voltage. No breakdown was observed on these devices meaning they can likely tolerate higher voltages and switch higher currents. In order to examine the high electric-field effects, switches fabricated with a small gap size should be used to reduce the effect of micropipes.¹⁶

In conclusion, planar PCSS have been fabricated on high-resistivity 4H-SiC in large sized structures. Photoconductivity measurements were done on these samples at bias voltages up to 1005 V. The average on-state resistance was 20Ω and the average off-state resistance was $5 \times 10^{12} \Omega$, for an on/off ratio of 2.5×10^{11} . The AFM image showed good surface morphology, atomic layer flatness, and large step width. The PCSS were measured with dc bias and showed repeatable behavior over many thousands of pulses.

This work was performed under USAF SBIR Contract No. F33615-02-M-2250 and benefited from programs at VCU from AFOSR, ONR, and NSF.

¹S. Nakashima, H. Matsunami, S. Yoshida, and H. Harima, *Silicon Carbide and Related Materials, 1995*, Institute of Physics Conference Series No. 142 (IOP, Bristol, 1996).

²*Properties of Advanced Semiconductor Materials*, edited by M. E. Levinstein, S. L. Rumyantsev, and M. S. Shur (Wiley, New York, 2001).

³P. G. Neudeck, Institute of Physics Conference Series 141, San Diego, CA, 1994, pp. 1–6.

⁴J. W. Palmour, C. H. Carter, C. E. Weitzel, and K. J. Nordquist, *Mater. Res. Soc. Symp. Proc.* **339**, 133 (1994).

⁵R. R. Siergiej, R. C. Clarke, S. Sriram, A. K. Agarwal, R. J. Bojko, A. W. Morse, V. Balakrishna, M. F. Macmillan, A. A. Burk, and C. D. Brandt, *Mater. Sci. Eng., B* **61**, 9 (1999).

⁶*High Power Optically Activated Solid-State Switches*, edited by A. Rosen and F. Zutavern (Artech House, Boston, 1994).

⁷N. E. Islam, E. Schumiloglu, and C. B. Fleddermann, *Appl. Phys. Lett.* **73**, 1988 (1998).

⁸T. S. Sudarshan, G. Gradinaru, G. Korony, W. Mitchell, and R. H. Hopkins, *Appl. Phys. Lett.* **67**, 3435 (1995).

⁹P. S. Cho, J. Goldhar, C. H. Lee, S. E. Sadow, and P. Neudeck, *J. Appl. Phys.* **77**, 1591 (1995).

¹⁰S. E. Sadow, P. S. Cho, J. Goldhar, J. Palmour, and Chi H. Lee, *Proc. SPIE* **1873**, 110 (1993).

¹¹S. E. Sadow, P. S. Cho, J. Goldhar, F. Barry McLean, J. W. Palmour, and C. H. Lee, *Inst. Phys. Conf. Ser.* **137**, 573 (1994).

¹²S. Sheng, M. G. Spencer, X. Tang, P. Zhou, K. Wongchotigul, C. Taylor, and G. L. Harris, *Mater. Sci. Eng., B* **46**, 147 (1997).

¹³N. Onojima, J. Suda, and H. Matsunami, *Appl. Phys. Lett.* **80**, 76 (2001).

¹⁴O. Kordina, P. Bergman, C. Hallin, and E. Janzen, *Appl. Phys. Lett.* **69**, 679 (1996).

¹⁵V. E. Chelnokov, A. L. Syrkin, and V. A. Dmitriev, *Diamond Relat. Mater.* **6**, 1480 (1997).

¹⁶G. Gradinaru and T. S. Sudarshan, *J. Appl. Phys.* **73**, 7643 (1993).